JOC The Journal of Organic Chemistry

Article

pubs.acs.org/joc

A Computational Study on Lewis Acid-Catalyzed Diastereoselective Acyclic Radical Allylation Reactions with Unusual Selectivity Dependence on Temperature and Epimer Precursor

Miglena K. Georgieva and A. Gil Santos*

REQUIMTE, CQFB, Departamento de Química, Faculdade de Ciências e Tecnologia, Universidade Nova Lisboa, 2829-516 Caparica, Portugal

Supporting Information

ABSTRACT: In stereoselective radical reactions, it is accepted that the configuration of the radical precursor has no impact on the levels of stereoinduction, as a prochiral radical intermediate is planar, with two identical faces, independently of its origin. However, Sibi and Rheault (*J. Am. Chem. Soc.* **2000**, *122*, 8873−8879) remarkably obtained different selectivities in the trapping of radicals originated from two epimeric bromides, catalyzed by chelating Lewis acids. The selectivity rationalization was made on the basis of different conformational properties of each epimer. However, in this paper we show that the two epimers have similar conformational properties, which implies that the literature proposal is unable to explain the experimental results. We propose an alternative mechanism, in which the final selectivity is dependent on different reaction rates for radical formation from each epimer. By introducing a different perspective of the reaction mechanism, our model also allows the rationalization of different chemical yields obtained from each epimer, a result not rationalized by the previous model. Adaptation to other radical systems, under different reaction conditions, is also possible.

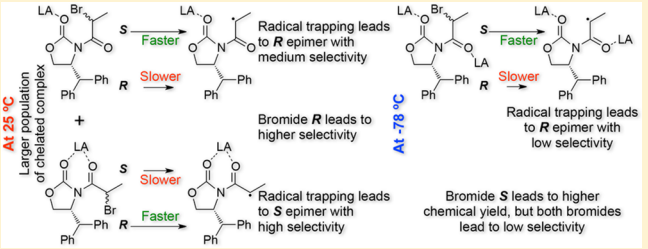

INTRODUCTION

Chiral auxiliaries are well-known units used in the induction of chirality in ionic reactions.[1] Several synthetic and mechanistic studies have been reported,[2] and steric and electrostatic effects are accepted to be the major influences determining the observed selectivities.[3] In many cases, the chiral auxiliary is connected to the substrate through an amide bond, which has a large impact on the selectivity of these systems.[3,4] Following their enormous success in ionic transformations, chiral auxiliaries have also been extensively used in the formation of carbon−carbon bonds under radical conditions, which has considerably increased their importance in organic chemistry.[5]

Radical carbon−carbon bond formation in acyclic systems, with high selectivity, has been a subject of investigation by many researchers.[5] The first reports mainly described synthetic methodologies,[5a−o] but recently, several mechanistic rationalizations have also been discussed by modern theoretical approaches.[4,5o−u] The general accepted idea in free radical chemistry is that the radical precursor configuration has little or no impact on the levels of stereoinduction in diastereoselective transformations, because a prochiral radical intermediate is generally planar or slightly tetrahedral and thus has two identical faces, independently of the radical precursor.[6] This fact, allied to the high conformational flexibility of acyclic systems, usually renders acyclic free radical reactions as nonselective processes. However, rotamer control by chelation with Lewis acids (LAs), associated with the use of chiral auxiliaries as inductors of stereoselectivity, can lead to very interesting results. On the basis of this approach, Sibi and collaborators published two remarkable experimental reports[6] on the stereoselectivity induction in radical allylation reactions (Table 1), in which high chemical yields and selectivities were obtained.

The main results obtained by Sibi and Rheault[6a] are presented in Table 1. The most important conclusions are that in the absence of LA or with LAs that do not allow the formation of chelates, the observed selectivities are very low, with slight excesses of isomer *R*. With LAs that can form chelated complexes, high selectivities were observed, the *S* epimer being preferentially formed. At the same time, with chelating LAs, higher selectivities were obtained at higher temperatures, the effect being more evident when more reactive (R = CO_2Me) trapping agents were used. Finally, higher selectivities were observed when the starting bromide was the *R* epimer, the effect being also more prominent when more reactive trapping agents were used.

The results above-described are unexpected, not only because the reaction selectivities usually improve with the reduction of temperature but also because the initial bromide should not influence the final selectivity. Indeed, as stated previously, the radical formed by bromide removal shall be planar, or slight tetrahedral, with very low inversion energy, and thus both epimers should form identical radicals which, in turn, should originate similar selectivities.

Received: September 11, 2014
Published: November 6, 2014

Table 1. Main Results Obtained by Sibi and Rheault[6a]

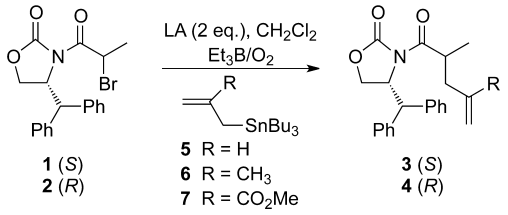

entry	Lewis Acid	reagent	temp (°C)	time (h)	R	yield[a] (%)	3:4
1	none	**1**, **2**	−78	3	H	93	1:1.8 (35.7:64.3)
2	$BF_3{\cdot}OEt_2$	**1**, **2**	−78	2.5	H	85	1:1.4 (41.2:58.8)
3	$MgBr_2$	**1**, **2**	−78	2	H	94	39:1 (97.5:2.5)
4	$MgBr_2$	**2**	−78	2	H	70	39:1 (97.5:2.5)
5	$MgBr_2$	**1**	−78	2	H	91	39:1 (97.5:2.5)
6	$MgBr_2$	**2**	RT	2	H	82	>50:1 (>98.0:2.0)
7	$MgBr_2$	**1**	RT	2	H	88	>50:1 (>98.0:2.0)
8	$MgBr_2$	**2**	−78	2	Me	78	24:1 (96.0:4.0)
9	$MgBr_2$	**1**	−78	2	Me	92	12:1 (92.3:7.7)
10	$MgBr_2$	**2**	RT	2	Me	75	>50:1 (>98.0:2.0)
11	$MgBr_2$	**1**	RT	2	Me	95	30:1 (96.8:3.2)
12	$MgBr_2$	**2**	−78	2	CO_2Me	25 (50)	3:1 (75.0:25.0)
13	$MgBr_2$	**1**	−78	2	CO_2Me	90 (10)	1:1 (50.0:50.0)
14	$MgBr_2$	**2**	RT	2	CO_2Me	80	40:1 (97.6:2.4)
15	$MgBr_2$	**1**	RT	2	CO_2Me	68 (27)	20:1 (95.2:4.8)

[a]Yield of isolated product and, in parentheses, yield of recovered starting material.

Scheme 1. Reaction Pathways Proposed by Sibi and Rheault[6a] To Rationalize the Observed Selectivity as well as Its Dependence on Temperature and Starting Epimeric Bromide

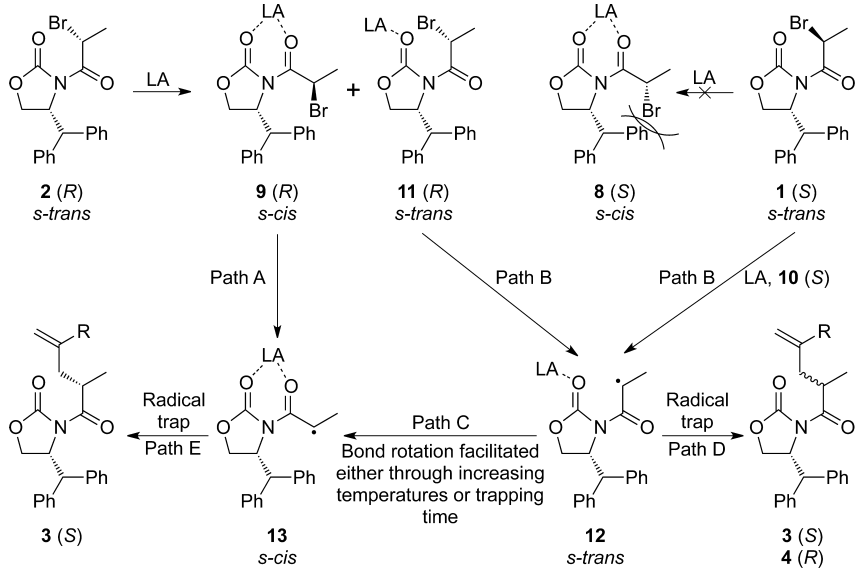

To rationalize the unexpected results, Sibi and Rheault proposed a general mechanism, as described in Scheme 1, in which almost all data are properly justified.[6a] Therefore, epimeric bromides **1** (*S*) and **2** (*R*) can bond the LA to form two possible types of complexes: complexes at the ring carbonyl group, in which the two carbonyl groups keep s-trans orientation (**10** and **11**), and chelated complexes, in which the two carbonyl groups adopt s-cis orientation (**8** and **9**). If the radical is formed from nonchelated bromides (**12**, path B), then the attack of the trapping agent shall happen at both faces, as the radical has low rigidity, and the selectivity will be low (path D). On the other hand, if the radical is formed from a chelated complex (**13**, path A), its conformation will be very rigid and the trapping agent shall preferentially attack at the opposite face of the ring substituent, thus leading to high selectivity (path E).

The selectivity dependence on temperature can be justified if the equilibrium between s-trans and s-cis conformers is slow at lower temperatures. Under these conditions, high amounts of nonchelated complexes shall exist (**10** and **11**), leading to lower selectivities (paths B and D). Temperature dependence is less notorious with lower reactive trapping agents, because they allow enough time for conformational change from s-trans to s-cis (**12** to **13**) radical complexes (path C). Therefore, while with low reactive trapping agents the majority of the reacting radical

dx.doi.org/10.1021/jo502102s | J. Org. Chem. 2014, 79, 11483−11495

species are in chelated form (**13**), with high reactive trapping reagents there is no time for s-trans to s-cis equilibration, which results in lower selectivity (reactive radical species exist as a mixture of **12** and **13**). Finally, the selectivity dependence on the initial epimeric bromide can be rationalized if one considers that s-trans to s-cis equilibration does not take place with bromide **1** (*S*), due to strong steric interactions between the bromine atom and the auxiliary ring substituent (**1**(*S*) → **8**(*S*), in Scheme 1). This means that radical formation via bromide **1** has to occur before chelate formation (path B), thus increasing the probability of trapping of s-trans forms (**12**), which results in lower selectivity (path D).

The reaction mechanism proposed by Sibi and Rheault, summarized above, is very interesting and quite reasonable. However, recent advances in the field of ionic asymmetric reactions, with oxazolidinones and imidazolidinones as chiral auxiliaries, force us to question some aspects of the proposed mechanism. Indeed, several theoretical studies have shown that both isomers (**1** and **2**) have very similar energies,[2g,3] either in s-cis or s-trans conformations, which implies that the rationalization of the different selectivities obtained when starting the reaction from the *R* and *S* epimers is, probably, not correct. Recent studies also show that high selectivities can be obtained with LA-complexed oxazolidinones as chiral auxiliaries, that keep the two carbonyl groups in s-trans orientation (nonchelated complexes).[3a] Finally, complexation energies are strongly dependent on several factors, which can make any selectivity rationalization a complex issue that needs experimental[7] and theoretical evaluation.[3]

Aiming at a positive contribution to the rationalization of the results reported by Sibi and Rheault,[6a] we envisaged a detailed computational study of their chemical system, and we concluded that while their proposal is appropriated in many aspects, it also needs the introduction of important corrections. Indeed, to fully rationalize the different selectivities obtained from each epimer, a model is necessary that accounts for the kinetics of radical formation starting from each isomer. Such a model also allows the rationalization of other interesting and important experimental observations that were not contemplated by the previous proposal.

RESULTS AND DISCUSSION

Selectivity Induction by Chelated and Nonchelated Radicals. According to the mechanism proposed in the literature,[6a] in the presence of $MgBr_2$, a chelating LA, the reaction can occur via a radical monocomplex at the ring carbonyl group (**12**, Scheme 1), in which the two carbonyl groups orient in s-trans conformation, or via a radical chelated complex (**13**, Scheme 1), in which the two carbonyl groups orient in s-cis conformation. Addition of radical traps to radical **13** originates very high selectivity, with preferential formation of the *S* epimer, while addition to radical **12** leads to low selectivity, with preferential formation of *R* epimer (Scheme 1 and Table 1). The authors also concluded that in the presence of nonchelating LAs, the reaction occurs via radical **12**, thus leading to low selectivity, with preferential formation of the *R* epimer (Table 1, entry 2). Finally, addition to radicals formed in the absence of LA also originates low selectivity, with preferential formation of the *R* epimer (Table 1, entry 1).

To evaluate the literature proposal[6a] and to validate the theoretical methods used in this work, we calculated complexed radicals **12** and **13** and noncomplexed radical **14** (Figure 1), as well as all possible transition state (TS) structures for addition of

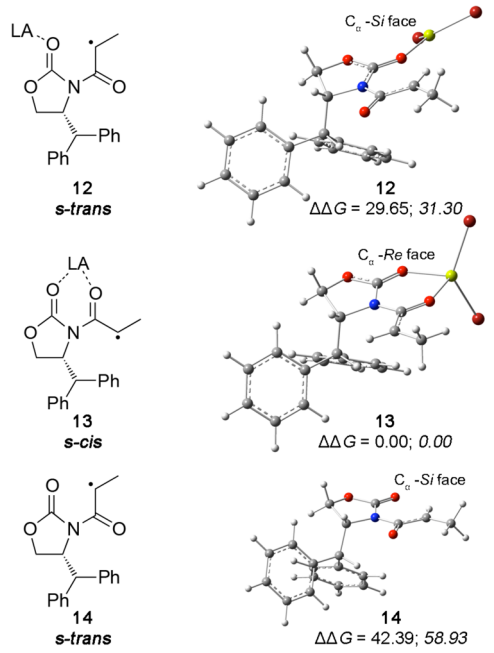

Figure 1. Most stable calculated structures of LA complexed radicals **12** and **13** and noncomplexed radical **14**. Gibbs energy values are relative to complex **13**. All energy values are in kJ mol^{-1} (PCM (U)PBE0/6-311G(d,p)//PCM (U)B3LYP/6-311G(d,p). In plain text are values calculated at room temperature, while values calculated at −78 °C are in italic.

allyltrimethylstannane (Figure 2). This radical trap was used instead of allyltributylstannane, for simplification of the model.

When calculating selectivities resulting from trapping of radical structures, we realized that while optimizations with different functionals and with basis sets of different ζ values originated coherent and similar results, extremely random results were sometimes obtained when basis sets with larger ζ values were used to calculate single points (sp) of structures optimized with smaller ζ values, either with the same or different functionals. Therefore, we ran optimizations with several functionals, with the larger basis set we could afford, 6-311G(d,p), followed by single point (sp) calculations with basis sets with the same ζ, and with or without extra diffuse functions. The obtained results are compiled in the Supporting Information (Tables S5 and S6) and indicate that all tested methods originate comparable selectivities, in good agreement with the experimental data. Therefore, considering the relative performance of all tested methods, the following discussion is based on sp calculations with PBE0/6-311G(d,p), over optimized structures with B3LYP/6-311G(d,p). Results obtained with other functionals and other basis sets are given in the Supporting Information.

As predicted in the literature,[6a] the radicals are planar, which means that the two epimeric bromides originate identical structures (Figure 1). Therefore, the selectivity obtained in the radical trapping step shall be independent of the initial epimer precursor, as stated in the experimental paper.[6a]

While all selectivities discussed below are calculated by Boltzmann averaging of the activation energies of several TS structures with different conformations (see the Supporting Information, Tables S7 and S8), Figure 2 only shows the most stable conformation of each TS. Rotation at bond $C^{1'}$–$C^{2'}$ (marked in **TS-1**) is not considered, as the resulting conformers

dx.doi.org/10.1021/jo502102s | J. Org. Chem. 2014, 79, 11483−11495

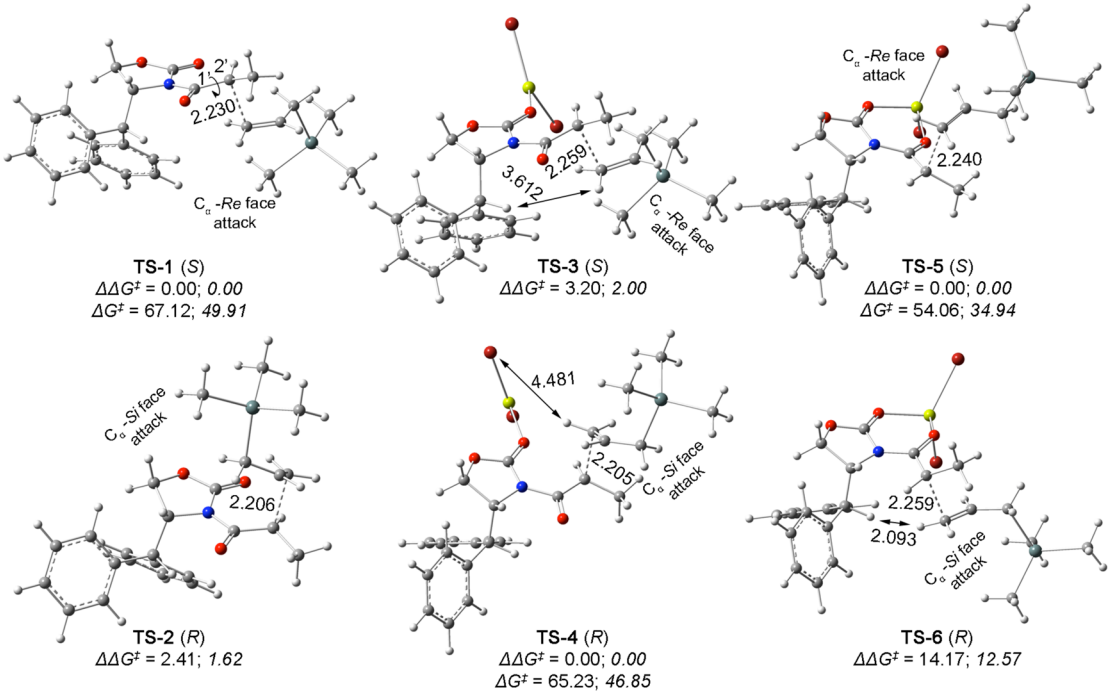

Figure 2. Most stable calculated TS structures for addition of allyltrimethylstannane to radicals **12**−**14**. Activation energy values are relative to the respective radical and allyltrimethylstannane. All energy values are in kJ mol^{-1} (PCM (U)PBE0/6-311G(d,p)//PCM (U)B3LYP/6-311G(d,p)). In plain text are values calculated at room temperature, while values calculated at −78 °C are in italic. Bond lengths and contact distances are in angstroms.

are too unstable (over 18 kJ mol^{-1}, see the Supporting Information).

The results presented in Figure 2 indicate that addition to noncomplexed radical **14** (**TS-1** and **TS-2**) leads to no selectivity (50.1:49.9 and 50.3:49.7 at, respectively, 25 °C and −78 °C). The selectivity calculated with M06-2X is slightly higher (40:60 and 34:66 at, respectively, 25 °C and −78 °C, with preferential formation of the *R* epimer: attack at the C$_\alpha$-si face, see the Supporting Information, Table S5), a result in very good agreement with the experiment (36:64, at −78 °C, Table 1, entry 1). When the reactive species is the radical monocomplexed at the ring carbonyl group **12** (**TS-3** and **TS-4**), the attack occurs preferentially at C$_\alpha$-si face, originating *R* product in moderate selectivity (15:85 and 12:88 at, respectively, 25 °C and −78 °C). Finally, when the reactive species is chelated radical **13** (**TS-5** and **TS-6**), attack occurs preferentially at C$_\alpha$-re face, originating *S* product in high selectivity (99.8:0.2 and 100:0 at, respectively, 25 °C and −78 °C).

With exception of the selectivity calculated for trapping of radical **12** (**TS-3** and **TS-4**, Figure 2), which is predicted to be too high (12:88 at −78 °C, with preferential formation of *R* epimer), when compared with the experimental values (no selectivity at −78 °C), the data presented in the previous paragraph are in quite good agreement with the experimental results. However, the rationalization of the calculated selectivities is substantially different from that proposed by Sibi and Rheault.[6a] Indeed, these authors justified the selectivity based on a previous model proposed by Evans and collaborators[8] for selectivity rationalization in Diels−Alder reactions.[9] Thus, according to Sibi and Rheault,[6a] the chelated s-cis orientation of carbonyl groups (**13**) is a rigid structure that leads to high selectivity, owing the strong differentiation of the two diastereofaces. Attack occurs preferentially at C$_\alpha$-re face, the opposite face of the chiral auxiliary substituent, thus leading to preferential formation of products with *S* configuration (**TS-5**, Figure 2). On the other hand, nonchelated s-trans conformations, being very flexible structures, originate two similar diastereofaces, thus leading to almost no selectivity. However, the analysis of the TS structures in Figure 2 shows that all of them have the auxiliary five-membered ring and the radical side chain in coplanar orientation. This means that there is no reduction of steric contacts by any type of adjustment or mobility of the side chain, as this would also reduce the electron delocalization to the carbonyl groups, thus increasing the global energy. Therefore, differences in calculated selectivities between chelated and nonchelated complexes are not resulting from different side-chain flexibility, as proposed in the literature,[6a] but just from different distances between the attacking alkene and the auxiliary substituent (Figure 2). Owing to the triangular planar configuration of the carbon atom of the amide group, the amide rotation puts the α carbon atom at different distances from the auxiliary substituent, thus considerably changing the steric interactions between this group and the attacking olefin (Figure 2). Steric interactions are maximized when the two carbonyl groups have s-cis orientation (chelated complex), which leads to an energy difference of ca. 12.6 kJ mol^{-1} between **TS-5** and **TS-6**, while a difference of only 2.0 kJ mol^{-1} is calculated between **TS-3** and **TS-4** (Figure 2). The difference in selectivity calculated between monocomplexed TSs (**TS-3** and **TS-4**) and noncomplexed structures (**TS-1** and **TS-2**) is mainly due to an electrostatic interaction between the attacking radical trap and one of the bromine atoms of the LA. This interaction, marked in **TS-4**, renders this structure considerably more stable than **TS-3**, while in the absence of LA, the selectivity results only from steric contacts between the attacking radical trap and the substituent at the chiral auxiliary. As stated above, this interaction is efficient only when the two carbonyl groups are in s-cis orientation (chelated complex).

Conformational Analysis of Complexed and Noncomplexed Structures. To evaluate the literature proposal[6a]

dx.doi.org/10.1021/jo502102s | J. Org. Chem. 2014, 79, 11483−11495

on the selectivity dependence on temperature and epimer precursor, a full conformational analysis of all species involved in the process had to be envisaged. We did the conformational analysis of the free epimeric bromides, of their complexes, and also of the resulting radicals.

The calculated thermodynamics for the conformational equilibria of bromides **1** (*S*) and **2** (*R*) are shown in Scheme 2

Scheme 2. Calculated Thermodynamics for the Conformational Equilibria of Uncomplexed Epimeric Bromides 1 and 2[a]

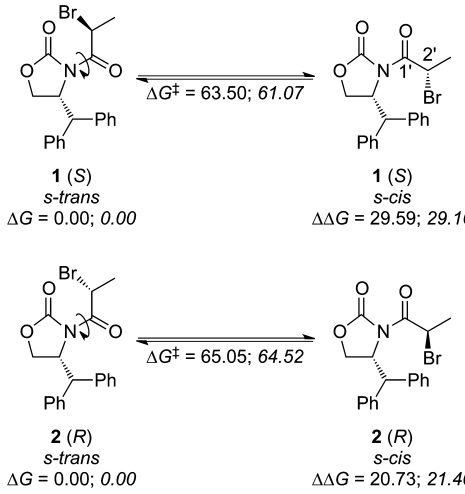

[a]Because two directions for amide-bond rotation are possible, energies are reported to the lowest calculated activation energy value and are relative to the s-trans conformation of each epimer. All energy values are in kJ mol^{-1} (PCM (U)PBE0/6-311G(d,p)//PCM (U)B3LYP/6-311G(d,p). In plain text are values calculated at room temperature, while values calculated at −78 °C are in italic.

(rotation at bond $C^{1\prime}-C^{2\prime}$ originates very unstable conformations, >19 kJ mol^{-1}, and is not considered in the following discussion; see the Supporting Information). In accordance with the literature,[2g,3,10] s-trans conformations are much more stable than their s-cis counterparts, either at −78 °C or at room temperature. On the other hand, the activation energy for s-trans to s-cis interconversion is slightly higher for the *R* epimer, independently of temperature. Therefore, albeit the slight difference in conformational equilibrium rates, due to the large energy difference between s-cis and s-trans conformations, in the range of experimental temperatures (25 °C to −78 °C), both epimers exist in s-trans conformation.

According to the mechanism proposed in the literature,[6a] when isomers **1** and **2** react with magnesium bromide, four possible complexes can be formed (monocomplexes at the ring carbonyl group, **10** and **11**, and chelated complexes **8** and **9**, Scheme 3). However, complexation at the chain carbonyl group can also occur (**15** and **16**) and, because the reaction is conducted in the presence of 2 equiv of LA,[6a] bis-complexes can also be formed, in which one molecule of LA is connected to each carbonyl group (**17** and **18**). In the following discussion all these possibilities are contemplated (Scheme 3).

According to the values in Scheme 3, chelated (**8** and **9**) and nonchelated monocomplexes at the ring carbonyl group (**10** and **11**) are stable in the range of temperatures experimentally used, the chelated forms being much more stable than nonchelated structures. On the other hand, monocomplexes at the chain carbonyl group (**15** and **16**) and bis-complexes (**17** and **18**) are only stable at low temperature. However, under the reaction conditions, monocomplexes at the chain carbonyl group (**15** and **16**) should never be formed in relevant amounts, as at any temperature they are less stable than all other complexes. Due to this, they will not be further considered along this discussion.

In disagreement with the proposal made by Sibi and Rheault,[6a] the data in Scheme 3 indicate that there is no important difference between the behaviors of the two epimers. The theoretical data indeed suggests that the chelated complex of the

Scheme 3. Calculated Complexation Energies (relative to reagents, LA = $MgBr_2$) of Epimeric Bromides 1 and 2, and Activation Energies for Amide-Bond Rotation[a]

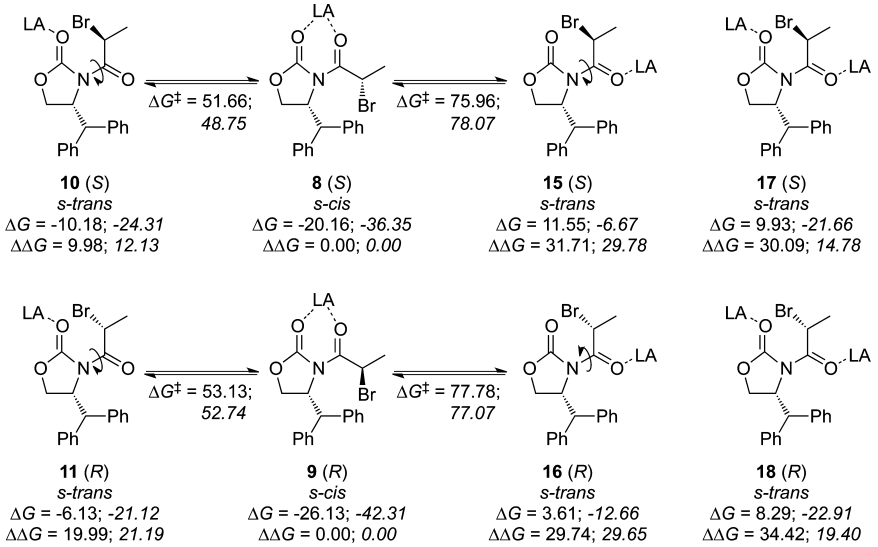

[a]Because amide-bond rotation can follow two different directions, energies are reported to the lowest calculated activation energy value and are relative to the respective s-trans conformation in each equilibrium. All energy values are in kJ mol^{-1} (PCM (U)PBE0/6-311G(d,p)//PCM (U)B3LYP/6-311G(d,p). In plain text are values calculated at room temperature, while values calculated at −78 °C are in italic.

dx.doi.org/10.1021/jo502102s | J. Org. Chem. 2014, 79, 11483−11495

R epimer (**9**) is slightly more stable than the chelated complex of *S* epimer (**8**, $\Delta G \approx 6.0$ kJ mol^{-1}, independently of temperature), and that the energy difference between monocomplexes at the ring carbonyl group and the respective chelated complexes is larger in the case of the *R* epimer (21.2 and 20.0 kJ mol^{-1}, between **11** and **9**, and 12.1 and 10.0 kJ mol^{-1}, between **10** and **8**, at −78 and 25 °C, respectively). However, both energy differences originate Boltzmann distributions of near 100%, in favor of chelated complexes. In addition, the activation energies for interconversion from open chain to chelated complexes (**10** to **8** and **11** to **9**), which are almost temperature independent, are 48.6 kJ mol^{-1} and 52.7 kJ mol^{-1} (at −78 °C) for, respectively, *S* and *R* epimers, indicating a faster interconversion of the *S* isomer (**10** to **8**) at this temperature (relative interconversion rate ≈11.7). At room temperature, the difference is smaller (≈ 1.5 kJ mol^{-1}) and is more or less irrelevant, as the relative interconversion rate is only ca. 1.8. Thus, according to our data, under similar reaction conditions, chelated complexes can be formed from both epimers.

Comparison between the activation energy values for amide-bond rotation, in Schemes 2 and 3, clearly shows that while complexation at the ring carbonyl group reduces the activation energy for bond rotation (reduction of double-bond character of the amide bond), the complexation at the chain carbonyl group does the opposite. Therefore, both thermodynamic and kinetic values suggest that, at room temperature, complexation at the ring carbonyl group should initially occur (formation of **10** and **11**), followed by amide-bond rotation to form chelated complexes **8** and **9**. At −78 °C, a mixture of bis-complexes (**17** and **18**) and monocomplexes at the ring carbonyl group (**10** and **11**) is expected, as soon as LA is added. We were unable to calculate activation energies for amide-bond rotation starting from bis-complexes **17** and **18**. However, considering the effect that monocomplexation at the chain carbonyl group has in the activation energies for amide-bond rotation, we expect the activation energy values for rotation in bis-complexes to be quite higher than those calculated for monocomplexes at the ring carbonyl group. Therefore, at −78 °C, any amide-bond rotation shall take place, at a very low rate, in monocomplexes at the ring carbonyl group (**10** and **11**), thus leading to chelated complexes **8** and **9**. This means that s-cis bis-complexes shall never be formed, either at high or at low temperature. Because of this, they are not considered in this discussion.

Conformational Analysis of Complexed Radicals. The selectivity dependence on temperature and trapping rate was rationalized by Sibi and Rheault[6a] as being correlated with the conformational interconversion rate between radical **12** and radical **13** (Scheme 1). We calculated the activation energy for amide-bond rotation, and the results are in Scheme 4.

The comparison between the values in Schemes 2, 3, and 4 reveals that while, at −78 °C, the activation energy for amide-bond rotation of uncomplexed bromides **1** and **2** is ca. 63 kJ mol^{-1} (Scheme 2), it is reduced to ca. 50 kJ mol^{-1} in bromide complexes (approximated value for **10** to **8** and **11** to **9** interconversions, Scheme 3), and to only ca. 31 kJ mol^{-1} in the radical structure (**12** to **13**, Scheme 4). If the difference calculated between the complexes and the radical is more or less irrelevant at room temperature, it becomes very important at −78 °C, as the rotation rate in the radical becomes ca. 100 000 times faster than in the complex precursors, thus allowing amide-bond rotation when less reactive radical traps are used, as proposed in the literature.[6a]

Scheme 4. Calculated Thermodynamics for the Conformational Equilibria of Monocomplexed Radicals (LA = $MgBr_2$)[a]

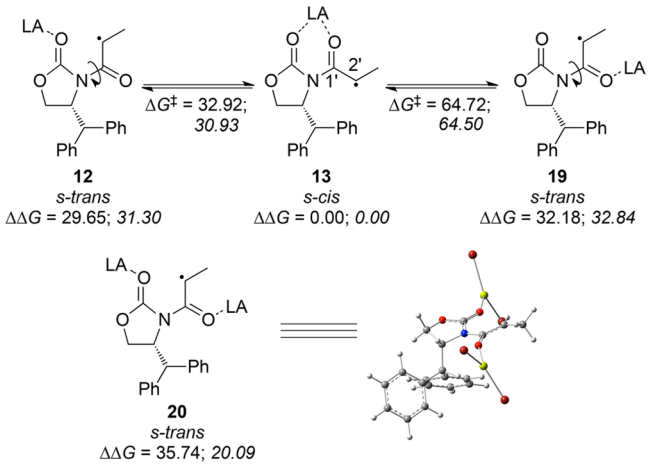

[a]Because two directions for amide-bond rotation are possible, energies are reported to the lowest calculated activation energy value and are relative to the respective s-trans conformation in each equilibrium. All energy values are in kJ mol^{-1} (PCM (U)PBE0/6-311G(d,p)//PCM (U)B3LYP/6-311G(d,p). In plain text are values calculated at room temperature, while values calculated at −78 °C are in italic.

Besides chelated radical **13** and monocomplexed radical **12** (Figure 1 and Scheme 4), we shall also consider the participation of radical **20** (Scheme 4), as it can be formed, at low temperatures, from complexes **17** and **18** (Scheme 3). As previously discussed for radicals **12** and **13**, radical **20** is also planar, which means that both epimeric precursors lead to a single structure. We were unable to find a TS structure for amide-bond rotation in radical **20**. However, we could determine that the activation energy for amide-bond rotation in radical **19** (a radical that shall never be formed, as its bromide precursor is always too unstable; see the discussion above) is twice the activation energy value for rotation in radical **12** (Scheme 4). Thus, considering the effect that complexation at the chain carbonyl group has in the activation energy for amide-bond rotation, it is reasonable to conclude that the rotation energy in radical **20** has to be quite higher than that calculated for radical **12**. Therefore, at −78 °C, the interconversion rate between the the s-trans form of radical **20** and its s-cis counterpart has to be an irrelevant process, by comparison with the interconversion rate between **12** and **13.**

Based on the data discussed so far, several important conclusions can be retrieved. In agreement with the model proposed by Sibi and Rheault,[6a] the reaction selectivity is controlled by the type of complexed radical that is being trapped, and chelated complexed radicals can, indeed, lead to vey high selectivity. As the activation energies for amide-bond rotation, either in bromine complexes **10** and **11** (Schemes 1 and 3) or in radical **12** (Schemes 1 and 4) are high, amide-bond rotation shall be a very slow process at low temperature. Therefore, at low temperature only low amounts of chelated complexes can be formed, which results in lower selectivity. However, as complexed radical **12** has much lower activation energy for amide-bond rotation (Scheme 4) than the respective complexed bromide precursors **10** and **11** (Scheme 3), with low reactive trapping agents, radical **12** has time enough to undergo amide-

dx.doi.org/10.1021/jo502102s | J. Org. Chem. 2014, 79, 11483−11495

Scheme 5. Proposed General Radical Cycle

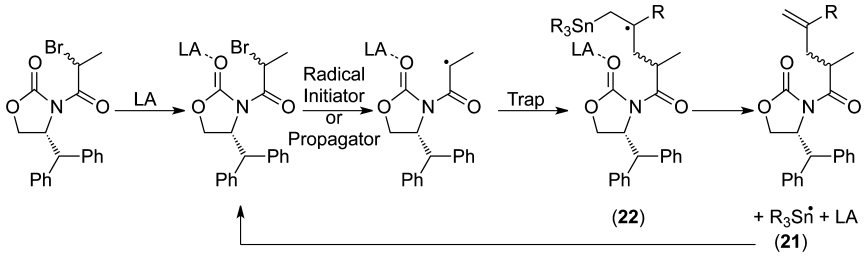

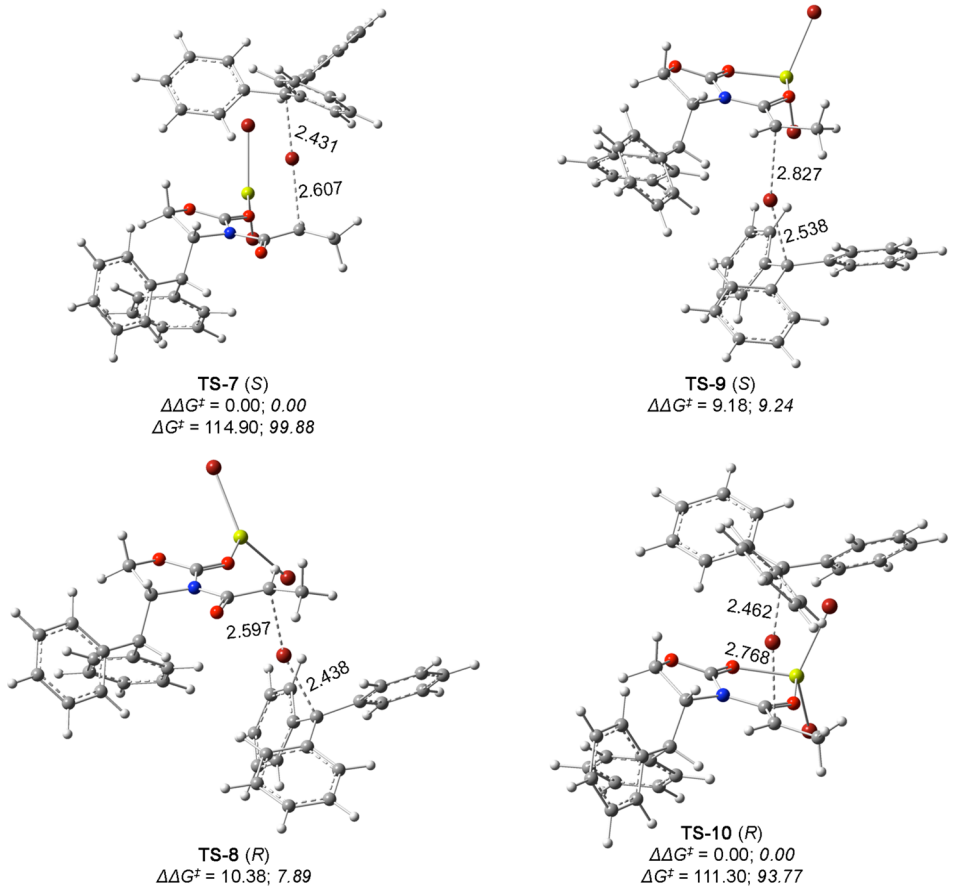

Figure 3. Calculated TS structures for bromine abstraction by triphenylmethyl radical, from complexes **8**–**11**. Gibbs energy values are relative to the respective complex and triphenylmethyl radical. All energy values are in kJ mol^{-1} (PCM (U)PBE0/6-311G(d,p)//PCM (U)B3LYP/6-31G(d,p). In plain text are values calculated at room temperature, while values calculated at −78 °C are in italic. Bond lengths are in angstroms.

bond rotation, thus leading to selectivity higher than that obtained with high reactive trapping agents.

In disagreement with the model proposed by Sibi and Rheault,[6a] the selectivity calculated for trapping of radical **12** (**TS-3** and **TS-4**, Figure 2) is predicted to be too high (12:88 at −78 °C, with preferential formation of the *R* epimer), when compared with the experimental values (no selectivity at −78 °C). On the other hand, besides monocomplexes **10** and **11**, and chelated complexes **8** and **9**, bis-complexes **17** and **18** also have to be considered when the reaction is conducted at low temperature (Scheme 3). Under such conditions, radical **20** (Scheme 4) can also be formed, and the overall selectivity has to result from attacks at radicals **12**, **13**, and **20** (Scheme 4). Finally, the two epimeric bromides, either uncomplexed (Scheme 2) or complexed (Scheme 3), are calculated as having very similar conformational behaviors, thus not justifying the different selectivities experimentally observed in reactions starting from one or the other epimer. Therefore, albeit the partial good agreement with the experimental data and with some aspects of the model proposed by Sibi and Rheault,[6a] our results fail to support other important aspects of the same model, which means that an alternative proposal is needed.

Proposal of an Alternative Model. If the two epimeric bromides originate the same radical, after radical formation, any reactivity differentiation resulting from the configuration of the initial radical precursors is impossible. Therefore, different behaviors observed for radicals resulting from epimeric bromides have to be traced back to the bromide precursors themselves. The only rationalization we can conceive is that the selectivity dependence on epimeric bromides results from different activation energies for radical formation from each one of the epimeric bromides. In other words, if the two epimers have different activation energies for radical formation, and if this difference is dependent on the epimers' conformation, then we

dx.doi.org/10.1021/jo502102s | J. Org. Chem. 2014, 79, 11483−11495

Scheme 6. Global Reaction Mechanism That Allows the Rationalization of All Experimental Data Obtained at Room Temperature (LA = $MgBr_2$)

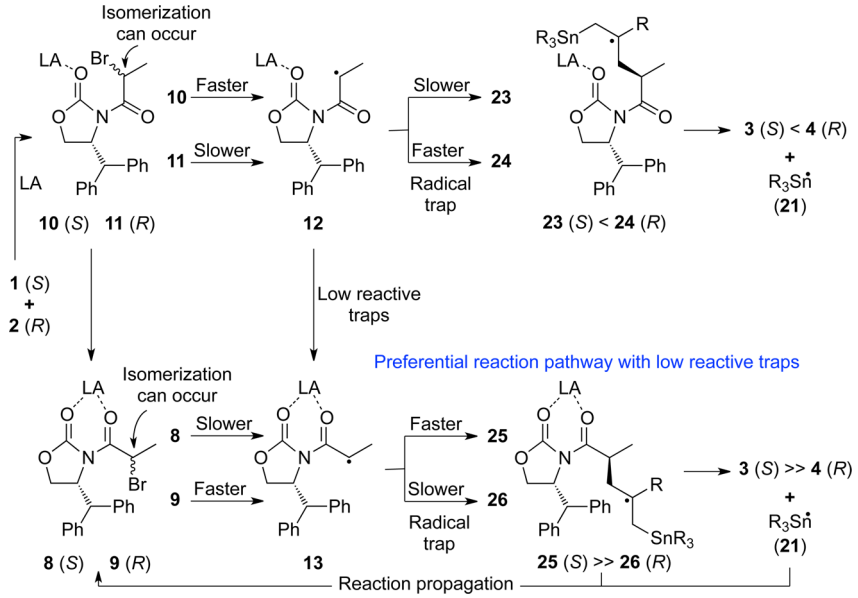

should be able to explain the selectivity dependence on the starting epimeric bromide.

After the initial radical formation by the radical initiator, the reaction has to be propagated by tin radicals (**21**), eventually formed by homolytic cleavage of radical intermediate **22**, as depicted in Scheme 5. Despite all our attempts, we were unable to find TS structures for bromine abstraction by trimethyltin or tributyltin radicals, as the process is very exothermic (>140 kJ mol^{-1}) and no energy increase was observed when scanning the bonds involved in the process (see the Supporting Information, Figure S1). Therefore, we decided to use triphenylmethyl radical, as it is quite stable and should allow us to obtain relative energies for bromine abstraction of both epimers in s-cis and s-trans conformations. However, even with this radical, we were only able to calculate TS structures for bromine abstraction with (U)B3LYP/6-31G(d,p), as with larger basis sets the imaginary frequencies become too small and some TSs fail to converge to proper structures. Similar failures were obtained when other functionals were used in these optimizations. Results obtained for bromine removal from complexes **8**–**11** (Scheme 3) are in Figure 3.

The relative energies shown in Figure 3 indicate that with triphenylmethyl radical, the step of bromine abstraction is, indeed, dependent on the epimer and also on its conformation. Because of steric interactions between the attacking radical and the substituent at the chiral auxiliary moiety, when the bromide complexes are in s-trans conformation (**TS-7** and **TS-8**), the *S* epimer reacts faster than the *R* epimer. The opposite is true when the bromides are in the form of chelated complex (**TS-9** and **TS-10**).

On the basis of the results discussed so far, we can propose an alternative model to justify the experimental data obtained by Sibi and Rheault.[6a] At room temperature, only complexes **8**–**11** are formed (Scheme 6). However, as the equilibrium between s-trans and s-cis conformations is fast ($\Delta G^{\ddagger} \approx 50$ kJ mol^{-1}, Scheme 3), both radicals **12** and **13** can be formed but with large excess of the chelated form **13**. If high reactive traps are used (Table 1, entries 14 and 15), radicals **12** and **13** are trapped as soon as they are formed but, owing to the excess of radical **13**, overall selectivity is high, albeit not maximal. On the other hand, if low reactive traps are used (Table 1, entries 6 and 7), radical **12**, formed from complexes **10** and **11**, has time to interconvert to radical **13** ($\Delta G^{\ddagger} \approx 30$ kJ mol^{-1}, Scheme 4), thus leading to maximum selectivity.

At −78 °C, complexes **10**, **11**, **17**, and **18** are formed (Scheme 7). At this temperature, the conformational equilibrium between s-trans and s-cis conformations is very slow ($\Delta G^{\ddagger} \approx 50$ kJ mol^{-1}, Scheme 3), which means that radicals **12** and **20** are formed and can both be trapped. We already concluded that the selectivity resulting from addition to radical **12** (**TS-3** and **TS-4**, Figure 2) is calculated to be substantially high (12:88, or even 5:95, with M06-2X; see the Supporting Information, Table S5), with preferential formation of the *R* epimer, a result in disagreement with the experimental data (no selectivity with high reactive traps, Table 1, entries 12 and 13, and ca. 98:2, with preferential formation of the *S* epimer, when low reactive traps are used, Table 1, entries 4 and 5). Therefore, we can anticipate that at low temperatures the reaction shall proceed mainly via radical **20**, and that this radical has to induce very low selectivity. We calculated the selectivity obtained by trapping of radical **20** with allyltrimethylstannane, and the results are in Figure 4, **TS-11** and **TS-12**. Figure 4 also shows TS structures calculated for bromine abstraction from bis-complexes **17** and **18** (**TS-13** and **TS-14**).

The comparison of the activation energy values for radical formation from complexes **10** and **11** (ca. 100 kJ mol^{-1}, **TS-7** and **TS-8**, Figure 3) with those calculated for radical formation from complexes **17** and **18** (ca. 80 kJ mol^{-1}, **TS-13** and **TS-14**, Figure 4) indicates that if the two complexes exist in equilibrium, radicals shall be preferentially formed from complexes **17** and **18** (Scheme 7). On the other hand, if radicals **12** and **20** are formed, the addition of the radical trapping agent shall preferentially occur with radical **20** ($\Delta G^{\ddagger} \approx 47$ kJ mol^{-1}, for trapping of radical **12**, Figure 2, **TS-3** and **TS-4**, and $\Delta G^{\ddagger} \approx 28$ kJ mol^{-1}, for trapping of radical **20**, Figure 4, **TS-11** and **TS-12**). Finally, the values in Figure 4 indeed indicate that the addition of the radical trap to radical **20** (**TS-11** and **TS-12**) leads to low selectivity (34:66 and 27:73 at, respectively, 25 °C and −78 °C), with

dx.doi.org/10.1021/jo502102s | J. Org. Chem. 2014, 79, 11483−11495

Scheme 7. Global Reaction Mechanism That Allows the Rationalization of All Experimental Data Obtained at Low Temperature (LA = $MgBr_2$)

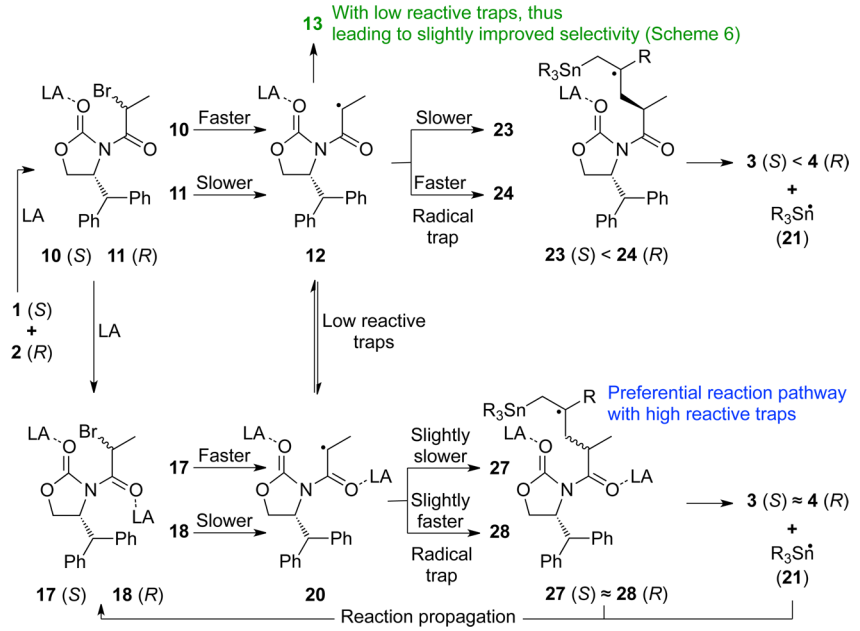

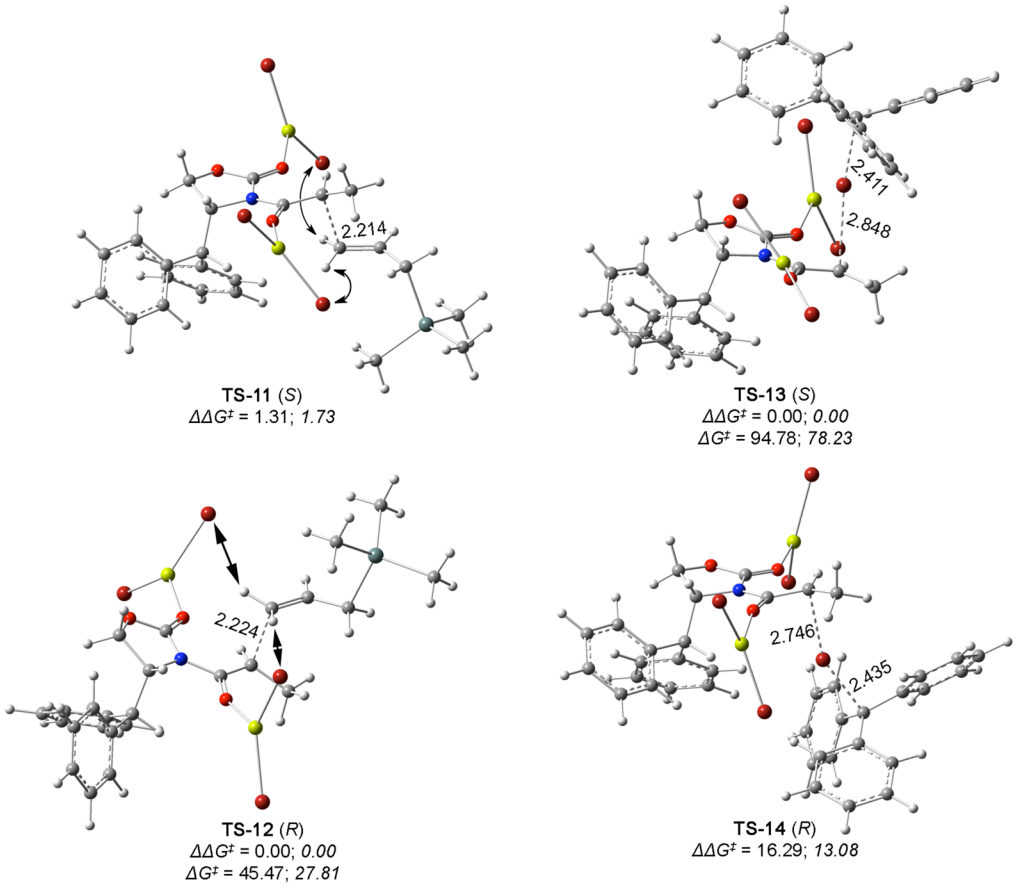

Figure 4. Most stable calculated TS structures for the addition of allyltrimethylstannane to radical **20** (left, **TS-11** and **TS-12**), and calculated TS structures for bromine abstraction by triphenylmethyl radical, from complexes **17** and **18** (right, **TS-13** and **TS-14**, respectively). Gibbs energy values for structures **TS-11** and **TS-12** have been calculated with PCM (U)PBE0/6-311G(d,p)//PCM (U)B3LYP/6-311G(d,p) and are relative to the respective radical and allyltrimethylstannane, while Gibbs energy values for structures **TS-13** and **TS-14** have been calculated with PCM (U)PBE0/6-311G(d,p)//PCM (U)B3LYP/6-31G(d,p) and are relative to the respective complex and triphenylmethyl radical. All energy values are in kJ mol^{-1}. In plain text are values calculated at room temperature, while values calculated at −78 °C are in italic. Bond lengths are in angstroms.

dx.doi.org/10.1021/jo502102s | J. Org. Chem. 2014, 79, 11483−11495

preferential formation of the *R* epimer. The energy difference obtained with M06-2X is even smaller, originating almost null selectivity (46:54 and 44:56 at, respectively, 25 °C and −78 °C), with preferential formation of the *R* epimer (see the Supporting Information, Table S5). The origin of this small value is the large distance between the attacking group and the chiral auxiliary substituent (carbonyl groups in s-trans orientation; see discussion above), and the similar steric and electrostatic interactions between the LA moieties and the trapping agent, when it attacks either at one or the other diastereoface (Figure 4).

On the basis of the results discussed in the previous paragraph, we can conclude, as predicted previously, that, at low temperatures, the reaction shall proceed via radical **20**, leading to low selectivity. However, if low reactive radical traps are used, radical **20** can equilibrate with radical **12**, which, owing to the low energy for amide-bond rotation ($\Delta G^{\ddagger} \approx 30$ kJ mol^{-1}, Scheme 4), can interconvert to radical **13** (Schemes 6 and 7). The result is an improvement on the reaction selectivity when low reactive traps are used (Table 1, entries 4 and 5), by comparison with the values obtained with high reactive traps (Table 1, entries 12 and 13).

Different behaviors observed between the two epimers, when the reaction is conducted with high reactive trapping agents, result from different reactivity for bromine abstraction (Schemes 6 and 7 and Figures 3 and 4). While the *R* epimer preferentially reacts to form radicals when in chelated form (**9** → **13**, **TS-9** and **TS-10**, Scheme 6 and Figure 3), the *S* epimer preferentially forms radicals from nonchelated structures (**10** → **12**, **TS-7** and **TS-8**, Schemes 6 and 7 and Figure 3, and **17** → **20**, **TS-13** and **TS-14**, Scheme 7 and Figure 4). Therefore, if radical formation occurs when chelated and nonchelated complexes coexist (at higher temperature amide-bond rotation before radical formation can occur), the *R* epimer preferentially reacts as chelated complex and originates higher selectivity (Scheme 6), while the *S* epimer preferentially reacts as nonchelated complex and leads to lower selectivity. The data in Table 1 indicate that even at −78 °C there is a small amount of amide-bond rotation before radical formation, as the selectivity obtained when starting from the *R* epimer is 75:25, while it is 1:1 when the reagent is the *S* epimer (Table 1, entries 12 and 13). These relative values can be explained, because any small amount of *R* chelated complex will preferentially react to form the radical, thus resulting in a small but clearly accounted selectivity. On the other hand, as the *S* epimer reacts faster in nonchelated conformation (s-trans) and slower in chelated conformation (s-cis), small amounts of chelated complex that can exist due to amide-bond rotation before radical formation will be unimportant, as the reaction will mainly occur via s-trans conformation (bis-complexed radical, **20**, Scheme 7), thus leading to low selectivity.

With low reactive traps, radicals formed in s-trans conformation have time to interconvert to the chelated (s-cis) form (**12** to **13**, Schemes 6 and 7), which means that both epimers shall originate similar selectivities, independently of temperature (Table 1, entries 4 to 7).

The model discussed above allows the rationalization of almost all data reported by Sibi and Rheault.[6a] However, it was experimentally observed that, despite originating lower selectivities, isomer *S* originates, in almost all cases, higher chemical yields. This difference becomes more evident when high reactive radical traps and low reaction temperatures are used. At −78 °C, the trapping with compound **7** (Table 1, entry 12) of radicals originated from the *R* epimer, leads only to 25% yield (50% recovery of starting material), while the *S* epimer leads, under similar reaction conditions, to 90% yield (Table 1, entry 13). Interestingly, with the same radical trap, but at room temperature, this relation inverts, with the *R* epimer leading to 80% yield (Table 1, entry 14), while the *S* epimer leads only to 68% yield (27% recovery of starting material, Table 1, entry 15). While Sibi and Rheault[6a] did not rationalize this observation, as their model does not allow it, our proposal does.

At low temperature, the complexes mainly exist as monocomplexes **10** and **11**, and bis-complexes **17** and **18**, in s-trans conformation (Scheme 7). Therefore, the *R* epimer (complexes **11** and **18**) reacts slower (higher activation energy), while the *S* epimer (complexes **10** and **17**) reacts faster (lower activation energy). This means that the radical propagation step is more efficient with the *S* epimer, which results in higher chemical yield when this isomer is used. On the other hand, at room temperature there is a large amount of chelated complex (complexes **8** and **9**, Scheme 6), which is a faster reactive species when the configuration is *R* (complex **9**) and a slower reactive species when the configuration is *S* (complex **8**). Therefore, the radical propagation step is more efficient with the *R* epimer, and the result is an important increase in the chemical yield of the reaction with this epimer, while a small reduction of chemical yield is observed in the reaction with the *S* counterpart. The effect is more important at lower temperature because of two different reasons. On one hand, as the activation energy difference between **TS-13** and **TS-14** is larger (13.1 kJ mol^{-1}, Figure 4), it originates a relative reaction rate of ca. 3000 (*S* epimer reacts faster), at −78 °C, while the smaller activation energy difference between **TS-9** and **TS-10** (9.2 kJ mol^{-1}, Figure 3) originates a relative reaction rate of only ca. 40 (*R* epimer reacts faster), at room temperature. On the other hand, while at low temperature there is almost no epimerization under the reaction conditions,[6a] at room temperature the epimerization occurs at an appreciable rate. Thus, at room temperature, the less reactive epimer *S*, in chelated form, can isomerize to configuration *R*, thus apparently leading to higher chemical yield.

Albeit justifying the relative chemical yields and diastereoselectivities obtained when a specific radical trap is used, the above model does not explain the difference in chemical yields obtained when different radical traps are used at similar temperatures. Indeed, if the radical propagator is tin radical **21** (Schemes 5−7), and as this species is identical no matter the radical trapping agent from which it is formed, one should expect differences of chemical yields with temperature, as discussed above, but, for similar temperatures, different radical traps should originate identical chemical yields. However, the experimental results show, for instance, chemical yields of 70% and 91%, with compound **5** as radical trap (Table 1, entries 4 and 5), and 25% and 90%, with compound **7** as radical trap (Table 1, entries 12 and 13), at −78 °C, for reactions starting from, respectively, *R* and *S* epimers. At room temperature, the results are also different, as shown in Table 1 (82% and 88%, entries 6 and 7, and 80% and 68%, entries 14 and 15, respectively). A possible explanation for these results can be the relative stabilization and activation energy for homolytic cleavage of radical intermediates **23** to **28** (Schemes 6 and 7) that result from different radical traps. Indeed, while compound **5** (Table 1) is a low reactive radical trap, it forms less stable radical intermediates **23** to **28** (radical intermediates formed from radical trap **5** are ca. 40 to 80 kJ mol^{-1} more energetic than intermediates formed from trap **7**; see the Supporting Information, Table S10). On the other hand, the activation energy for homolytic cleavage of intermediates originated from trap **5** is ca. 20 to 40 kJ mol^{-1} lower than the activation energy for cleavage of intermediates resulting from

dx.doi.org/10.1021/jo502102s | J. Org. Chem. 2014, 79, 11483−11495

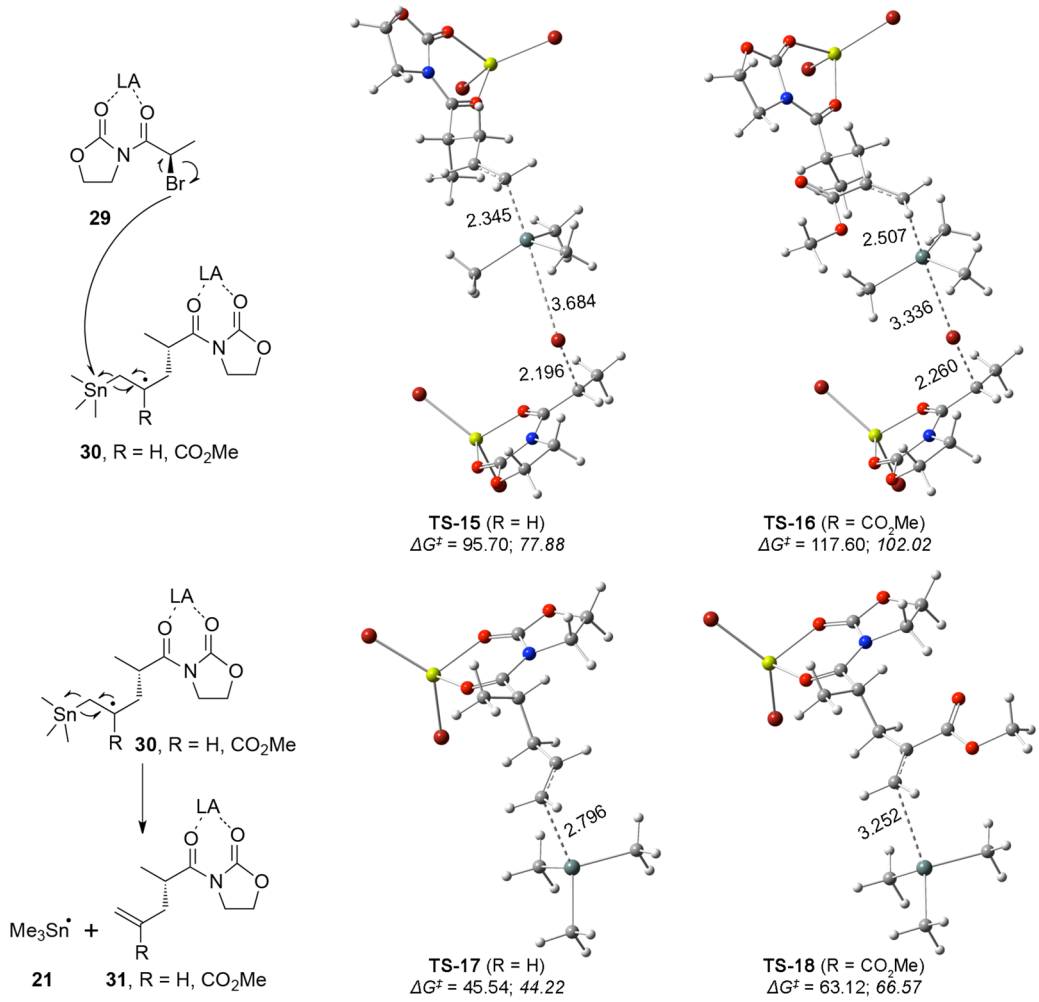

Figure 5. Calculated TS structures for bromine abstraction from a simplified chelated complex (**29**) by intermediate radical **30**, a simplified version of intermediate radical **25** (*S*), and comparison with the respective homolytic cleavage to form radical propagator **21** (LA = $MgBr_2$). Gibbs energy values are relative to the bromide complex and the respective radical intermediate, or just to the radical intermediate, respectively. All energy values are in kJ mol^{-1} (PCM (U)PBE0/6-311G(d,p)//PCM (U)B3LYP/6-311G(d,p). In plain text are values calculated at room temperature, while values calculated at −78 °C are in italic. Bond lengths are in angstroms.

trap **7** (see the Supporting Information, Table S11). Therefore, radical intermediates **23** to **28** formed from compound **7** at low temperature can be stable enough to reduce the formation of radical propagator **21**, thus lowering the reaction yield.

An alternative explanation can be conceived if radical intermediates **23** to **28** (Schemes 6 and 7), formed from the reactive radical trapping agent **7** (Table 1), not only suffer homolytic cleavage to form radical propagator **21** but also act as radical propagators, by directly removing the bromine atom from the reagent (Schemes 6 and 7). In this case, different species would propagate the reaction when different radical trapping agents are used. Such a mechanism would originate not only different selectivities but also different chemical yields at different temperatures, between low reactive and high reactive radical trapping agents, as experimentally observed.

As the chemical structures involved in such a mechanism are very large and impossible to calculate with the theoretical models used throughout this study, we calculated simplified structures, as shown in Figure 5, using either compound **5** or compound **7** as radical trapping agents. Despite our attempts, we could only obtain TS structures for chelated complexes, which are less relevant for the evaluation of our proposal. Indeed, chelated complexes exist mainly at room temperature, where both traps behave similarly. At low temperature, when larger differences are observed, radical formation shall occur mainly from bis-complexes. In any case, the values shown in Figure 5 indicate that such a mechanism is indeed possible, albeit with higher activation energies (ca. 34 kJ mol^{-1} between **TS-15** and **TS-17**, and ca. 35 kJ mol^{-1} between **TS-16** and **TS-18**) than those calculated for the formation of radical propagator **21** (bottom structures in Figure 5). To support our proposal, the reaction starting from bis-complexed radicals with radical trap **7** (R = CO_2Me) needs to have a different relationship of energies between the two possible mechanisms, thus favoring the concerted process (top mechanism in Figure 5) at low temperature. Because of hardware limitations, this issue will be addressed in future work.

■ CONCLUSIONS

The theoretical results discussed in this paper clearly show that the two epimeric bromides used by Sibi and Rheault[6a] have similar conformational and complexing properties. Therefore, the model proposed in the literature to rationalize the selectivity dependence on the epimeric bromide is not supported by our data. On the other hand, the theoretical data indicate that the

dx.doi.org/10.1021/jo502102s | J. Org. Chem. 2014, 79, 11483−11495

activation energy for radical formation depends on the complexed bromide configuration and also on its conformation. These results allow the rationalization of the selectivity dependence on the epimeric reagents, as well as the selectivity dependence on temperature, and the chemical yield dependence on epimeric bromide and reaction temperature. Thus, while the literature model only allowed the rationalization of part of the known experimental data, our proposed model, which introduces a different perspective on the reaction mechanism, allows the rationalization of all experimental results. The model adaptation to other radical systems, under different reaction conditions, is also possible.

COMPUTATIONAL METHODS

Full geometry optimizations have been performed with Gaussian 09, Revision B.01, software package,[11] employing density functional theory (DFT)[12] with the hybrid functional (U)B3LYP and the 6-311G(d,p) basis set (with LanL2DZ for Sn[13]), with exception of the structures in Figure 3 and **TS-13** and **TS-14** in Figure 4, which have been optimized with the 6-31G(d,p) basis set. Solvent effects in dichloromethane were included in the optimizations by using the polarizable continuum model (PCM).[14] Harmonic vibrational frequencies have been calculated for all located stationary structures to verify whether they are minima or transition states. Zero-point energies and thermal corrections have been taken from unscaled vibrational frequencies, and the wave functions were verified for spin contamination. Single-point PCM energy calculations, in dichloromethane, were performed at (U)PBE0/6-311G(d,p)[15] level of theory (with LanL2DZ for Sn), over the optimized PCM (U)B3LYP/6-311G(d,p) geometries, and are given in all tables and figures. Single-point PCM calculations, in dichloromethane, over the optimized structures have also been performed at (U)M06-2X/6-311G(d,p),[16] (U)M06-2X/6-311+G(d,p), and (U)B2PLYP/6-311G-(d,p)[17] levels of theory (with LanL2DZ for Sn), and the results are given in the Supporting Information. To validate the B3LYP optimizations, selected structures were also optimized with gas-phase (U)-BHandHLYP/6-311G(d,p),[12,18] PCM (U)BHandHLYP/6-311G(d,p), PCM (U)PBE0/6-311G(d,p), and PCM (U)M06-2X/6-311G(d,p), with LanL2DZ for Sn. All energies are in kJ mol^{-1} and were calculated at 25 °C (regular) and −78 °C (italic). All bond lengths and contact distances are in angstroms. The discussion is based on the results obtained with PCM (U)PBE0/6-311G(d,p)//PCM (U)B3LYP/6-311G(d,p).

ASSOCIATED CONTENT

Supporting Information

Cartesian coordinates, energies, and imaginary frequencies at PCM (U)B3LYP/6-311G(d,p), PCM (U)B3LYP/6-31G(d,p), gas-phase (U)BHandHLYP/6-311G(d,p), PCM (U)-BHandHLYP/6-311G(d,p), PCM (U)PBE0/6-311G(d,p), and PCM (U)M06-2X/6-311G(d,p). Sp energies at PCM (U)PBE0/6-311G(d,p), PCM (U)M06-2X/6-311G(d,p), PCM (U)M06-2X/6-311+G(d,p), and PCM (U)B2PLYP/6-311G(d,p), over optimized structures with PCM (U)B3LYP/6-311G(d,p). This material is available free of charge via the Internet at http://pubs.acs.org.

AUTHOR INFORMATION

Corresponding Author

*E-mail: ags@fct.unl.pt.

Notes

The authors declare no competing financial interest.

ACKNOWLEDGMENTS

We are grateful to the Fundação para a Ciência e Tecnologia (PTDC/QUI-QUI/104056/2008 and SFRH/BPD/22179/2005) for financial support.

REFERENCES

(1) (a) Blazis, V. J.; Koeller, K. J.; Spilling, C. D. *J. Org. Chem.* **1995**, *60*, 931−940. (b) Camps, P.; Perez, F.; Soldevilla, N.; Borrego, M. A. *Tetrahedron: Asymmetry* **1999**, *10*, 493−509. (c) Cardillo, G.; Gentilucci, L.; Gianotti, M.; Tolomelli, A. *Org. Lett.* **2001**, *3*, 1165−1167. (d) O'Meara, J. A.; Gardee, N.; Jung, M.; Ben, R. N.; Durst, T. *J. Org. Chem.* **1998**, *63*, 3117−3119.

(2) (a) Caddick, S.; Jenkins, K. *Tetrahedron Lett.* **1996**, *37*, 1301−1304. (b) Caddick, S.; Jenkins, K.; Treweeke, N.; Candeias, S. X.; Afonso, C. A. M. *Tetrahedron Lett.* **1998**, *39*, 2203−2206. (c) Kubo, A.; Kubota, H.; Takahashi, M.; Nunami, K. *J. Org. Chem.* **1997**, *62*, 5830−5837. (d) Caddick, S.; Afonso, C. A. M.; Candeias, S. X.; Hitchcock, P. B.; Jenkins, K.; Murtagh, L.; Pardoe, D.; Santos, A. G.; Treweeke, N. R.; Weaving, R. *Tetrahedron* **2001**, *57*, 6589−6605. (e) Poll, T.; Helmchen, G.; Bauer, B. *Tetrahedron Lett.* **1984**, *25*, 2191−2194. (f) Poll, T.; Metter, J. O.; Helmchen, G. *Angew. Chem., Int. Ed. Engl.* **1985**, *24*, 112−114. (g) Gnas, Y.; Glorius, F. *Synthesis* **2006**, 1899−1930. (h) Santos, A. G.; Candeias, S. X.; Afonso, C. A. M.; Jenkins, K.; Caddick, S.; Treweeke, N. R.; Pardoe, D. *Tetrahedron* **2001**, *57*, 6607−6614.

(3) (a) Bakalova, S. M.; Duarte, F. J. S.; Georgieva, M. K.; Cabrita, E. J.; Santos, A. G. *Chem.—Eur. J.* **2009**, *15*, 7665−7677. (b) Bakalova, S. M.; Santos, A. G. *J. Org. Chem.* **2004**, *69*, 8475−8481. (c) Santos, A. G.; Pereira, J.; Afonso, C. A. M.; Frenking, G. *Chem.—Eur. J.* **2004**, *11*, 330−343. (d) Bakalova, S. M.; Santos, A. G. *Eur. J. Org. Chem.* **2006**, 1779−1789. (e) Duarte, F. J. S.; Bakalova, S. M.; Cabrita, E. J.; Santos, A. G. *J. Org. Chem.* **2011**, *76*, 6997−7004.

(4) Georgieva, M. K.; Duarte, F. J. S.; Bakalova, S. M.; Santos, A. G. *Eur. J. Org. Chem.* **2010**, 4841−4850.

(5) (a) Curran, D. P.; Porter, N. A.; Giese, B. *Stereochemistry of Radical Reactions: Concepts, Guidelines and Synthetic Applications*; Wiley-VCH: Weinheim, 1996. (b) Sibi, M. P.; Porter, N. A. *Acc. Chem. Res.* **1999**, *32*, 163−171. (c) Porter, N. A.; Giese, B.; Curran, D. P. *Acc. Chem. Res.* **1991**, *24*, 296−304. (d) Sibi, M. P.; Manyem, S.; Zimmerman, J. *Chem. Rev.* **2003**, *103*, 3263−3295. (e) Yamamoto, Y.; Onuki, S.; Yumoto, M.; Asao, N. *J. Am. Chem. Soc.* **1994**, *116*, 421−422. (f) Porter, N. A.; Wu, J. H.; Zhang, G.; Reed, A. D. *J. Org. Chem.* **1997**, *62*, 6702−6703. (g) Murakata, M.; Jono, T.; Mizuno, Y.; Hoshino, O. *J. Am. Chem. Soc.* **1997**, *119*, 11713−11714. (h) Bazin, S.; Feray, L.; Vanthuyne, N.; Siric, D.; Bertrand, M. *Tetrahedron* **2007**, *63*, 77−85. (i) Bazin, S.; Feray, L.; Vanthuyne, N.; Bertrand, M. *Tetrahedron* **2005**, *61*, 4261−4274J. (j) Sibi, M. P.; Manyem, S. *Org. Lett.* **2002**, *4*, 2929−2932. (k) Cardinal-David, B.; Guérin, B.; Guindon, Y. *J. Org. Chem.* **2005**, *70*, 776−784. (l) Yang, D.; Zheng, B.-F.; Gu, S.; Chan, P. W. H.; Zhu, N.-Y. *Tetrahedron: Asymmetry* **2003**, *14*, 2927−2937. (m) Yang, D.; Yan, Y.-L.; Law, K.-L.; Zhu, N.-Y. *Tetrahedron* **2003**, *59*, 10465−10475. (n) Dakternieks, D.; Dunn, K.; Perchyonok, V. T.; Schiesser, C. H. *Chem. Commun.* **1999**, 1665−1666. (o) Zeng, L.; Dakternieks, D.; Duthie, A.; Perchyonok, V. T.; Schiesser, C. H. *Tetrahedron: Asymmetry* **2004**, *15*, 2547−2554. (p) Dakternieks, D.; Perchyonok, V. T.; Schiesser, C. H. *Tetrahedron: Asymmetry* **2003**, *14*, 3057−3068. (q) Um, J. M.; Gutierrez, O.; Schoenebeck, F.; Houk, K. N.; MacMillan, D. W. C. *J. Am. Chem. Soc.* **2010**, *132*, 6001−6005. (r) Fang, X.; Liu, K.; Li, C. *J. Am. Chem. Soc.* **2010**, *132*, 2274−2283. (s) Nakayama, R.; Matsubara, H.; Fujino, D.; Kobatake, T.; Yoshida, S.; Yorimitsu, H.; Oshima, K. *Org. Lett.* **2010**, *12*, 5748−5751. (t) Taaning, R. H.; Lindsay, K. B.; Schiøtt, B.; Daasbjerg, K.; Skrydstrup, T. *J. Am. Chem. Soc.* **2009**, *131*, 10253−10262. (u) Godin, F.; Prévost, M.; Viens, F.; Mochirian, P.; Brazeau, J.-F.; Gorelsky, S. I.; Guindon, Y. *J. Org. Chem.* **2013**, *78*, 6075−6103.

(6) (a) Sibi, M. P.; Rheault, T. R. *J. Am. Chem. Soc.* **2000**, *122*, 8873−8879. (b) Sibi, M. P.; Ji, J. *Angew. Chem., Int. Ed. Engl.* **1996**, *35*, 190−192.

(7) (a) Messmer, A. T.; Lippert, K. M.; Steinwand, S.; Lerch, E.-B. W.; Hof, K.; Ley, D.; Gerbig, D.; Hausmann, H.; Schreiner, P. R.; Bredenbeck, J. *Chem.—Eur. J.* **2012**, *18*, 14985−14995. (b) Messmer, A. T.; Lippert, K. M.; Schreiner, P. R.; Bredenbeck, J. *Phys. Chem. Chem. Phys.* **2013**, *15*, 1509−1517. (c) Messmer, A. T.; Steinwand, S.; Lippert, K. M.; Schreiner, P. R.; Bredenbeck, J. *J. Org. Chem.* **2012**, *77*, 11091−11095.
(8) Evans, D. A.; Chapman, K. T.; Bisaba, J. *J. Am. Chem. Soc.* **1988**, *110*, 1238−1256.
(9) Evans, D. A.; Helmchen, G.; Rüping, M. Auxiliary-Mediated Asymmetric Synthesis. In *Asymmetric Synthesis - The Essentials*, 2nd ed.; Christmann, M.; Bräse, S., Eds.; Wiley-VCH: Weinheim, 2007; pp 3 − 9.
(10) Taaning, R. H.; Lindsay, K. B.; Schiøtt, B.; Daasbjerg, K.; Skrydstrup, T. *J. Am. Chem. Soc.* **2009**, *131*, 10253−10262.
(11) Frisch, M. J.; Trucks, G. W.; Schlegel, H. B.; Scuseria, G. E.; Robb, M. A.; Cheeseman, J. R.; Scalmani, G.; Barone, V.; Mennucci, B.; Petersson, G. A.; Nakatsuji, H.; Caricato, M.; Li, X.; Hratchian, H. P.; Izmaylov, A. F.; Bloino, J.; Zheng, G.; Sonnenberg, J. L.; Hada, M.; Ehara, M.; Toyota, K.; Fukuda, R.; Hasegawa, J.; Ishida, M.; Nakajima, T.; Honda, Y.; Kitao, O.; Nakai, H.; Vreven, T.; Montgomery, J. A., Jr.; Peralta, J. E.; Ogliaro, F.; Bearpark, M.; Heyd, J. J.; Brothers, E.; Kudin, K. N.; Staroverov, V. N.; Kobayashi, R.; Normand, J.; Raghavachari, K.; Rendell, A.; Burant, J. C.; Iyengar, S. S.; Tomasi, J.; Cossi, M.; Rega, N.; Millam, J. M.; Klene, M.; Knox, J. E.; Cross, J. B.; Bakken, V.; Adamo, C.; Jaramillo, J.; Gomperts, R.; Stratmann, R. E.; Yazyev, O.; Austin, A. J.; Cammi, R.; Pomelli, C.; Ochterski, J. W.; Martin, R. L.; Morokuma, K.; Zakrzewski, V. G.; Voth, G. A.; Salvador, P.; Dannenberg, J. J.; Dapprich, S.; Daniels, A. D.; Farkas, O.; Foresman, J. B.; Ortiz, J. V.; Cioslowski, J.; Fox, D. J. *Gaussian 09, Revision B.01*; Gaussian, Inc., Wallingford, CT, 2009.
(12) (a) Koch, W.; Holthausen, M. C. *A Chemist's Guide to Density Functional Theory*, 2nd ed.; Wiley: New York, 2001. (b) Parr, R. G.; Yang, W. *Density Functional Theory of Atoms and Molecules*; Oxford University Press: Oxford, 1989.
(13) (a) Hay, P. J.; Wadt, W. R. *J. Chem. Phys.* **1985**, *82*, 270−83. (b) Wadt, W. R.; Hay, P. J. *J. Chem. Phys.* **1985**, *82*, 284−98. (c) Hay, P. J.; Wadt, W. R. *J. Chem. Phys.* **1985**, *82*, 299−310. (d) Paton, R. S.; Mackey, J. L.; Kim, W. H.; Lee, J. H.; Danishefsky, S. M.; Houk, K. N. *J. Am. Chem. Soc.* **2010**, *132*, 9335−9340. (e) Luft, J. A. R.; Winkler, T.; Kessabi, F. M.; Houk, K. N. *J. Org. Chem.* **2008**, *73*, 8175−8181.
(14) Tomasi, J.; Mennucci, B.; Cammi, R. *Chem. Rev.* **2005**, *105*, 2999−3093.
(15) (a) Perdew, J. P.; Burke, K.; Ernzerhof, M. *Phys. Rev. Lett.* **1996**, *77*, 3865. (b) Perdew, J. P.; Burke, K.; Ernzerhof, M. *Phys. Rev. Lett.* **1997**, *78*, 1396. (c) Adamo, C.; Barone, V. *J. Chem. Phys.* **1999**, *110*, 6158−6170. (d) Wheeler, S. E.; Moran, A.; Pieniazek, S. N.; Houk, K. N. *J. Phys. Chem. A* **2009**, *113*, 10376−10384.
(16) Zhao, Y.; Truhlar, D. G. *J. Phys. Chem. A* **2008**, *112*, 1095−1099.
(17) Grimme, S. *J. Chem. Phys.* **2006**, *124*, 034108.
(18) (a) Kyne, S. H.; Schiesser, C. H.; Matsubara, H. *J. Org. Chem.* **2008**, *73*, 427−434. (b) Horvat, S. M.; Schiesser, C. H. *New J. Chem.* **2014**, *38*, 2595−2603. (c) Kyne, S. H.; Schiesser, C. H.; Matsubara, H. *Org. Biomol. Chem.* **2011**, *9*, 3217−3224. (d) Kyne, S. H.; Schiesser, C. H.; Matsubara, H. *Org. Biomol. Chem.* **2007**, *5*, 3938−3943.